

Design of sensor networks for instantaneous inversion of modally reduced order models in structural dynamics^{☆,☆☆}

K. Maes^{a,*}, E. Lourens^{a,b}, K. Van Nimmen^{a,c}, E. Reynders^a, G. De Roeck^a, G. Lombaert^a

^a*KU Leuven, Department of Civil Engineering, Kasteelpark Arenberg 40, 3001 Leuven, Belgium*

^b*Delft University of Technology, Faculty of Civil Engineering and Geosciences, Stevinweg 1, 2628 CN Delft, The Netherlands*

^c*KAHO Sint-Lieven, Department of Industrial Engineering, Gebroeders De Smetstraat 1, 9000 Ghent, Belgium*

Abstract

In structural dynamics, the forces acting on a structure are often not well known. System inversion techniques may be used to estimate these forces from the measured response of the structure. This paper first derives conditions for the invertibility of linear system models that apply to any instantaneous input estimation or joint input-state estimation algorithm. The conditions ensure the identifiability of the dynamic forces and system states, their stability and uniqueness. The present paper considers the specific case of modally reduced order models, which are generally obtained from a physical, finite element model, or from experimental data. It is shown how in this case the conditions can be directly expressed in terms of the modal properties of the structure. A distinction is made between input estimation and joint input-state estimation. Each of the conditions is illustrated by a conceptual example. The practical implementation is discussed for a case study where a sensor network for a footbridge is designed.

Keywords: force identification, state estimation, system invertibility, stability, uniqueness, sensor network

1. Introduction

The dynamic forces acting on a structure and the corresponding system states are of great importance to many engineering applications. Often, however, the dynamic forces and resulting system states can hardly be obtained by direct measurements, e.g. for wind loads, and have to be determined indirectly from dynamic measurements of the system response using system inversion techniques.

Originally, force identification and state estimation problems were treated separately. Force identification problems were initially solved off-line in a deterministic setting. Many methods were proposed, most of them based on the inversion of the frequency response function [1, 2, 3] or making

[☆]*Postprint submitted to Mechanical Systems and Signal Processing*

^{☆☆}*Published version:* K. Maes, E. Lourens, K. Van Nimmen, E. Reynders, G. De Roeck, and G. Lombaert. Design of sensor networks for instantaneous inversion of modally reduced order models in structural dynamics *Mechanical Systems and Signal Processing*, 52-53:628-644, 2014. <http://dx.doi.org/10.1016/j.ymssp.2014.07.018>

*Corresponding author. Tel.: +32 16328669.

Email address: kristof.maes@bwk.kuleuven.be (K. Maes)

use of a time domain approach [4, 5, 6, 7]. Several state estimation algorithms have been proposed for linear as well as for non-linear systems [8, 9, 10, 11]. A recursive deterministic method was presented by Klinkov and Fritzen [12], estimating both the input and system states from a set of output measurements. Currently, the attention is shifted to the development of recursive combined deterministic-stochastic approaches [13, 14]. These methods do not only account for measurement errors, but also for modelling errors and additional unknown vibration sources. An algorithm was proposed by Gillijns and De Moor, where the input estimation is performed prior to the state estimation step [15]. The algorithm was introduced in structural dynamics by Lourens et al. [16], extending the algorithm for use with reduced-order models. A similar approach was proposed by Niu et al. [17]. Alternatively, the dynamic forces and system states can be jointly estimated using a classical Kalman filter, hereby including the unknown forces in an augmented state vector [18].

This paper focuses on instantaneous system inversion, i.e. inversion without any time delay, covering the majority of inversion algorithms applied in structural dynamics. The invertibility of a system in general depends on three conditions. Firstly, the dynamic forces and/or the corresponding states must be identifiable from the given set of response measurements. Secondly, the system inversion algorithm must be stable, such that small perturbations of the data do not give rise to unbounded errors on the identified quantities. Thirdly, the estimates obtained must be uniquely defined by the measurement data. In the literature, the main requirements on the system description for instantaneous invertibility are extensively documented for the general case of linear systems [19, 20, 21]. For the specific case of linear modally reduced order models, which are often used in structural dynamics, the general conditions can be directly translated into a number of requirements on the sensor network, i.e. sensor types, sensor locations, and number of sensors.

The outline of this paper is as follows. In Section 2, the problem of system inversion is outlined. Next, in Sections 3–5, the requirements on the sensor network are derived, starting from the general conditions for system invertibility, as given in the literature. Section 6 discusses the practical implementation of the requirements for a case study, where a sensor network for a footbridge is designed that allows for the identification of multiple forces on the bridge deck. Finally, in Section 7, the work is summarized.

2. Problem formulation

In structural dynamics, first principles models, e.g. finite element (FE) models, are widely used. In many cases, modally reduced order models are applied, constructed from a limited number of structural modes. When proportional damping is assumed, the continuous-time decoupled equations of motion for modally reduced order models are given by:

$$\ddot{\mathbf{z}}(t) + \mathbf{\Gamma}\dot{\mathbf{z}}(t) + \mathbf{\Omega}^2\mathbf{z}(t) = \mathbf{\Phi}^T\mathbf{S}_p(t)\mathbf{p}(t) \quad (1)$$

where $\mathbf{z}(t) \in \mathbb{R}^{n_m}$ is the vector of modal coordinates, with n_m the number of modes taken into account in the model. The excitation force is written as the product of a selection matrix $\mathbf{S}_p(t) \in \mathbb{R}^{n_{\text{dof}} \times n_p}$, specifying the force locations, and a time history vector $\mathbf{p}(t) \in \mathbb{R}^{n_p}$, with n_p the number of forces. For the remainder of this paper, the selection matrix $\mathbf{S}_p(t)$ is assumed to be time-invariant. The results, however, can be readily extended to the case where $\mathbf{S}_p(t)$ is varying with time. The number of degrees of freedom is denoted by n_{dof} . $\mathbf{\Gamma} \in \mathbb{R}^{n_m \times n_m}$ is a diagonal matrix containing the terms $2\xi_j\omega_j$ on its diagonal, where ω_j and ξ_j are the natural frequency and modal damping ratio corresponding to mode j , respectively. $\mathbf{\Omega} \in \mathbb{R}^{n_m \times n_m}$ is a diagonal matrix as well,

containing the natural frequencies ω_j on its diagonal, and $\Phi \in \mathbb{R}^{n_{\text{dof}} \times n_m}$ is a matrix containing the mass normalized mode shapes ϕ_j as columns. Throughout the paper it is assumed that the system does not contain rigid body modes, corresponding to a natural frequency $\omega_j = 0$ rad/s.

The decoupled governing equations can be written in state-space form, which after time discretization reads:

$$\mathbf{x}_{[k+1]} = \mathbf{A}\mathbf{x}_{[k]} + \mathbf{B}\mathbf{p}_{[k]} \quad (2)$$

where $\mathbf{x}_{[k]} = \mathbf{x}(k\Delta t)$, $\mathbf{p}_{[k]} = \mathbf{p}(k\Delta t)$, and $\mathbf{d}_{[k]} = \mathbf{d}(k\Delta t)$, $k = 1, \dots, N$, Δt is the sampling time step, and N is the total number of samples. The state vector $\mathbf{x}_{[k]}$ consists of the modal displacements and velocities:

$$\mathbf{x}_{[k]} = \begin{bmatrix} \mathbf{z}_{[k]} \\ \dot{\mathbf{z}}_{[k]} \end{bmatrix} \quad (3)$$

The specific form of \mathbf{A} and \mathbf{B} depends on the time discretization scheme and will not be further considered. The reader is referred to [22] for a detailed overview of common time discretization schemes. As an alternative to models based on first principles, models can be directly identified from experimental vibration data using system identification techniques, see e.g. [23].

The output vector is generally written as:

$$\mathbf{d}(t) = \mathbf{S}_{d,a}\Phi\ddot{\mathbf{z}}(t) + \mathbf{S}_{d,v}\Phi\dot{\mathbf{z}}(t) + \mathbf{S}_{d,d}\Phi\mathbf{z}(t) \quad (4)$$

where $\mathbf{S}_{d,a}$, $\mathbf{S}_{d,v}$, and $\mathbf{S}_{d,d} \in \mathbb{R}^{n_d \times n_{\text{dof}}}$ are selection matrices indicating the degrees of freedom corresponding to the acceleration, velocity and displacement or strain measurements, respectively. The output vector is composed of $n_{d,d}$ displacement or strain measurements, $n_{d,v}$ velocity measurements and $n_{d,a}$ acceleration measurements, where n_d is the sum of $n_{d,d}$, $n_{d,v}$, and $n_{d,a}$.

Eq. (4) is transformed into its state-space form, using Eq. (1):

$$\mathbf{d}_{[k]} = \mathbf{G}\mathbf{x}_{[k]} + \mathbf{J}\mathbf{p}_{[k]} \quad (5)$$

The expressions for the state-output matrix \mathbf{G} and the direct transmission matrix \mathbf{J} do in general not depend on the time discretization scheme, because Eqs. (4) and (5) do not involve a time lag. The expressions for \mathbf{G} and \mathbf{J} are given by:

$$\mathbf{G} = [\mathbf{S}_{d,d}\Phi - \mathbf{S}_{d,a}\Phi\Omega^2 \quad \mathbf{S}_{d,v}\Phi - \mathbf{S}_{d,a}\Phi\Omega], \quad \mathbf{J} = [\mathbf{S}_{d,a}\Phi\Phi^T\mathbf{S}_p] \quad (6)$$

When process noise and measurement noise are added to Eqs. (2) and (5), respectively, a discrete-time combined deterministic-stochastic state-space description of the system is obtained:

$$\mathbf{x}_{[k+1]} = \mathbf{A}\mathbf{x}_{[k]} + \mathbf{B}\mathbf{p}_{[k]} + \mathbf{w}_{[k]} \quad (7)$$

$$\mathbf{d}_{[k]} = \mathbf{G}\mathbf{x}_{[k]} + \mathbf{J}\mathbf{p}_{[k]} + \mathbf{v}_{[k]} \quad (8)$$

where $\mathbf{x}_{[k]} \in \mathbb{R}^{n_s}$ is the state vector, $\mathbf{d}_{[k]} \in \mathbb{R}^{n_d}$ is the output vector, assumed to be measured, and $\mathbf{p}_{[k]} \in \mathbb{R}^{n_p}$ is the unknown input vector. The deterministic system behaviour is described by the system matrices \mathbf{A} , \mathbf{B} , \mathbf{G} and \mathbf{J} . The process noise $\mathbf{w}_{[k]} \in \mathbb{R}^{n_s}$ and measurement noise $\mathbf{v}_{[k]} \in \mathbb{R}^{n_d}$ are not considered in what follows. In practice, when both process noise and measurement noise are present, the estimated forces and system states also depend on the noise processes. The invertibility

conditions presented in this paper are necessary but not sufficient for guaranteeing that the forces and system states can be identified in presence of noise.

In structural dynamics, the problem of input estimation consists of estimating the excitation forces $\mathbf{p}_{[k]}$, acting on a structure at known locations, from a set of response measurements $\mathbf{d}_{[k]}$. When joint input-state estimation is performed, the system states $\mathbf{x}_{[k]}$ and the excitation forces $\mathbf{p}_{[k]}$ are jointly estimated. Very often, unknown ambient forces such as wind loads are acting on the structure. For these loads, the force locations or spatial distributions of the forces are not well known. In this case, joint input-state estimation can be applied to identify a set of forces $\mathbf{p}_{[k]}$, acting at predefined locations, and the corresponding system states. The forces are then not the true forces acting on the structure but equivalent forces that compensate for any unknown source of vibration [16].

3. Identifiability conditions

System identifiability requires that the measured output contains information on the quantities that are estimated, i.e. system inputs and/or system states. This condition can be subdivided into two separate requirements, the observability requirement and the direct invertibility requirement, which are both discussed next.

3.1. Observability

System observability requires that all states are observed in the system output. In general, system observability is tested by means of the rank of the observability matrix \mathcal{O} :

$$\mathcal{O} \equiv \begin{bmatrix} \mathbf{G} \\ \mathbf{GA} \\ \vdots \\ \mathbf{GA}^{n_s-1} \end{bmatrix} \quad (9)$$

Theorem 3.1. *The system described by Eqs. (2) and (5) is observable if and only if $\text{rank}(\mathcal{O}) = n_s$, with n_s the number of system states.*

Proof. A proof can be found in [24]. □

When a modally reduced order model is used, system observability requires that all modes considered in the model contribute to the measured output. From the definition of the observability matrix in Eq. (9), and the definition of the output vector in Eq. (4), the observability test can be reformulated in terms of the modal characteristics.

Theorem 3.2. *The modally reduced order system described by Eqs. (2) and (5) is observable if and only if for all damped natural frequencies, with each damped natural frequency having multiplicity m_l (i.e. $\omega_{d,j} = \omega_{d,j+1} = \dots = \omega_{d,j+m_l-1}$), the following equation holds:*

$$\text{rank}((\mathbf{S}_{d,d} + \mathbf{S}_{d,v} + \mathbf{S}_{d,a})[\phi_j \quad \phi_{j+1} \quad \dots \quad \phi_{j+m_l-1}]) = m_l \quad (10)$$

where ϕ_j is the mass-normalized mode shape of mode j , and $\omega_{d,j} = \omega_j \sqrt{1 - \xi_j^2}$ is the damped natural frequency corresponding to mode j .

Proof. The proof proceeds from the decoupled form of the state-space model, as is outlined in Appendix A. The proof of Theorem 3.2 is given in Appendix B. \square

Corollary 3.1. *The modally reduced order system described by Eqs. (2) and (5) cannot be observable if the matrix*

$$\mathbf{S}_d \Phi = (\mathbf{S}_{d,d} + \mathbf{S}_{d,v} + \mathbf{S}_{d,a}) \Phi \quad (11)$$

contains any zero columns.

This follows directly from Theorem 3.2, since Eq. (10) cannot hold for all damped natural frequencies if $\mathbf{S}_d \Phi$ contains zero columns.

Proposition 3.1. *If all damped natural frequencies $\omega_{d,j}$ are different, the modally reduced order system described by Eqs. (2) and (5) is observable if and only if the matrix $\mathbf{S}_d \Phi$ does not contain zero columns.*

Proof. If all damped natural frequencies $\omega_{d,j}$ are different, then $m_l = 1$ in Eq. (10). In this case, the system is observable if and only if for all modes j the following equation holds:

$$\text{rank}((\mathbf{S}_{d,d} + \mathbf{S}_{d,v} + \mathbf{S}_{d,a})\phi_j) = 1 \quad (12)$$

where $(\mathbf{S}_{d,d} + \mathbf{S}_{d,v} + \mathbf{S}_{d,a})\phi_j \in \mathbb{R}^{n_d \times 1}$. This is true if at least one element of the column vector $(\mathbf{S}_{d,d} + \mathbf{S}_{d,v} + \mathbf{S}_{d,a})\phi_j$ is different from zero. Therefore, Eq. (12) is equivalent to imposing that column j of the matrix $\mathbf{S}_d \Phi$ is non-zero. Since Eq. (12) has to hold for all modes j , observability holds if and only if the matrix $\mathbf{S}_d \Phi$ does not contain zero columns. \square

In the case of pure input estimation, the system states as such are not of interest, and the observability requirement is of no direct importance. In the case of joint input-state estimation, both the forces and system states must be identifiable and observability is required.

3.2. Controllability

When unknown ambient forces are exciting the structure, the estimated forces are not the true forces but rather a set of forces that compensate for any source of vibration, as explained in Section 2. As these unknown vibration sources generally excite all modes, the forces to be estimated should be able to do so as well. This is equivalent to imposing system controllability, which requires that all states can be controlled by the system input.

In general, system controllability is tested by means of the rank of the controllability matrix \mathbf{C} :

$$\mathbf{C} \equiv [\mathbf{B} \quad \mathbf{AB} \quad \dots \quad \mathbf{A}^{n_s-1}\mathbf{B}] \quad (13)$$

Theorem 3.3. *The system described by Eqs. (2) and (5) is controllable if and only if $\text{rank}(\mathbf{C}) = n_s$, with n_s the number of system states.*

Proof. A proof can be found in [24]. \square

When a modally reduced order model is used, the controllability test can be formulated in terms of the modal characteristics.

Theorem 3.4. *The modally reduced order system described by Eqs. (2) and (5) is controllable if and only if for all damped natural frequencies, with each damped natural frequency having multiplicity m_l (i.e. $\omega_{d,j} = \omega_{d,j+1} = \dots = \omega_{d,j+m_l-1}$), the following equation holds:*

$$\text{rank}(\mathbf{S}_p^T [\phi_j \quad \phi_{j+1} \quad \dots \quad \phi_{j+m_l-1}]) = m_l \quad (14)$$

where ϕ_j is the mass-normalized mode shape of mode j , and $\omega_{d,j} = \omega_j \sqrt{1 - \xi_j^2}$ is the damped natural frequency corresponding to mode j .

Proof. The proof proceeds from the decoupled form of the state-space model, as is outlined in Appendix A. The proof of Theorem 3.4 is given in Appendix C. \square

Corollary 3.2. *The modally reduced order system described by Eqs. (2) and (5) cannot be controllable if the matrix $\mathbf{S}_p^T \Phi$ contains any zero columns.*

This follows directly from Theorem 3.4, since Eq. (14) cannot hold for all damped natural frequencies if $\mathbf{S}_p^T \Phi$ contains zero columns.

Proposition 3.2. *If all damped natural frequencies $\omega_{d,j}$ are different, the modally reduced order system described by Eqs. (2) and (5) is controllable if and only if the matrix $\mathbf{S}_p^T \Phi$ does not contain zero columns.*

Proof. If all damped natural frequencies $\omega_{d,j}$ are different, then $m_l = 1$ in Eq. (14). In this case, the system is controllable if and only if for all modes j the following equation holds:

$$\text{rank}(\mathbf{S}_p^T \phi_j) = 1 \quad (15)$$

where $\mathbf{S}_p^T \phi_j \in \mathbb{R}^{n_p \times 1}$. This is true if at least one element of the column vector $\mathbf{S}_p^T \phi_j$ is different from zero. Therefore, Eq. (15) is equivalent to imposing that column j of the matrix $\mathbf{S}_p^T \Phi$ is non-zero. Since Eq. (15) has to hold for all modes j , controllability holds if and only if the matrix $\mathbf{S}_p^T \Phi$ does not contain zero columns. \square

The concept of observability and controllability is illustrated by means of a conceptual example.

Example 3.1. Consider a steel beam with I-shaped cross section [18]. The beam has steel plates welded to its ends and is suspended on very flexible springs (Fig. 1). In this way, dynamic free-free boundary conditions are approximately obtained.

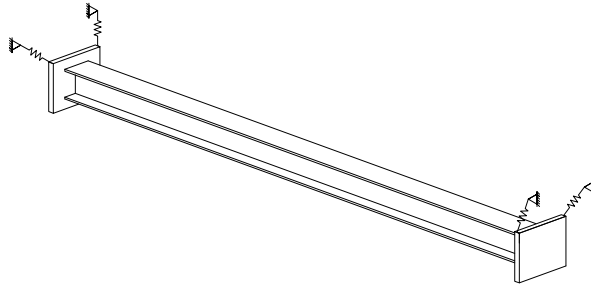


Fig. 1: Structure as considered for the illustration of the theoretical derivation, three dimensional view.

Assume a modally reduced order model constructed from two modes of the beam, one torsional mode (mode T1) and one vertical bending mode (mode B1), where both modes have a multiplicity

of one. A single vertical force, indicated as p_1 , is acting eccentrically on the beam (Fig. 2). The response of the structure is measured using one accelerometer, a_1 , placed on the beam axis. The force and sensor locations are shown in Fig. 2.

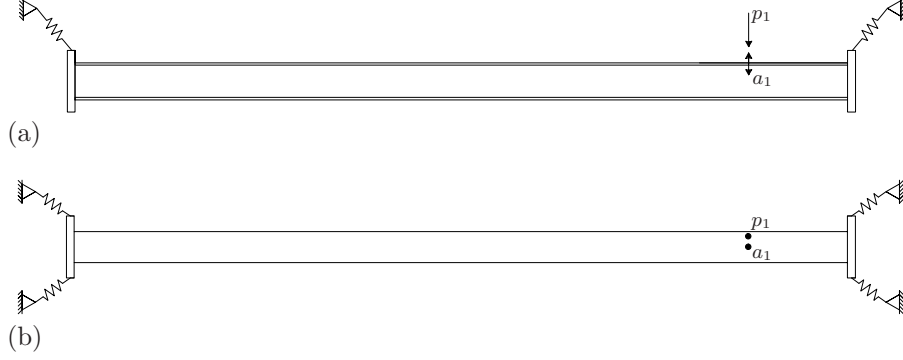


Fig. 2: Force and sensor locations as considered for Example 3.1, (a) side view and (b) top view.

Since only bending of the beam contributes to the measured acceleration response, it is clear that in general:

$$\mathbf{S}_d \Phi = \begin{bmatrix} \text{T1} & \text{B1} \\ 0 & * \end{bmatrix} \quad (16)$$

where $*$ indicates a non-zero number. Mode T1 is not observed by the sensor. The observability matrix \mathcal{O} will not have full column rank n_s ($= 2n_m = 4$) and the system is not observable.

The force p_1 excites both the vertical bending mode and the torsional mode. The matrix $\mathbf{S}_p^T \Phi$ becomes:

$$\mathbf{S}_p^T \Phi = \begin{bmatrix} \text{T1} & \text{B1} \\ * & * \end{bmatrix} \quad (17)$$

The matrix $\mathbf{S}_p^T \Phi$ has no zero columns. Therefore, since all modes have multiplicity one, the system is controllable.

3.3. Direct invertibility

Direct invertibility requires that the system input can be estimated from the output without a time delay, which is called instantaneous inversion. The necessary and sufficient condition for direct invertibility is extensively documented in the literature [20, 21], and is given by the following theorem.

Theorem 3.5. *The system described by Eqs. (2) and (5) is instantaneously invertible if and only if $\text{rank}(\mathbf{J}) = n_p$.*

Proof. A proof can be found in [20]. □

For modally reduced order models, this condition results in two important requirements which have to be taken into account when performing instantaneous system inversion. The first requirement is given in the following proposition:

Proposition 3.3. *The matrix \mathbf{J} ($= \mathbf{S}_{d,a} \Phi \Phi^T \mathbf{S}_p$) is of rank n_p only if $\text{rank}(\mathbf{S}_p^T \Phi) = n_p$. This also implies that the number of forces to be identified n_p cannot exceed the number of modes n_m .*

Proof. The rank of the product of two matrices $\mathbf{A}_1 \in \mathbb{R}^{n_1 \times n_2}$ and $\mathbf{A}_2 \in \mathbb{R}^{n_2 \times n_3}$ satisfies the following inequality [25]:

$$\text{rank}(\mathbf{A}_1 \mathbf{A}_2) \leq \min(\text{rank}(\mathbf{A}_1), \text{rank}(\mathbf{A}_2)) \quad (18)$$

with

$$\begin{aligned} \text{rank}(\mathbf{A}_1) &\leq \min(n_1, n_2), \\ \text{rank}(\mathbf{A}_2) &\leq \min(n_2, n_3) \end{aligned} \quad (19)$$

By replacing $\mathbf{A}_1 = \mathbf{S}_{d,a} \Phi$ and $\mathbf{A}_2 = \Phi^T \mathbf{S}_p$, it follows immediately from Eqs. (18) and (19) that \mathbf{J} is of rank n_p only if $\text{rank}(\mathbf{S}_p^T \Phi) = n_p$ and $n_p \leq n_m$. \square

This means that the forces must be able to control at least n_p modes independently, in order to be distinguishable.

Proposition 3.4. *The matrix \mathbf{J} ($= \mathbf{S}_{d,a} \Phi \Phi^T \mathbf{S}_p$) is of rank n_p only if $\text{rank}(\mathbf{S}_{d,a} \Phi) \geq n_p$. This implies that the number of acceleration measurements $n_{d,a}$ has to be larger than or equal to the number of forces n_p .*

Proof. By replacing $\mathbf{A}_1 = \mathbf{S}_{d,a} \Phi$ and $\mathbf{A}_2 = \Phi^T \mathbf{S}_p$, it follows immediately from Eqs. (18) and (19) that \mathbf{J} is of rank n_p only if $\text{rank}(\mathbf{S}_{d,a} \Phi) \geq n_p$ and $n_{d,a} \geq n_p$. \square

Example 3.2. Assume a modally reduced order model constructed from three modes of the beam, two torsional modes (modes T1 and T2) and one vertical bending mode (mode B1), with all modes having a multiplicity of one. Three vertical forces are acting on the beam, one of them eccentrically, two others centrically, indicated as p_1 , p_2 , and p_3 , respectively. The force locations are shown in Fig. 3.

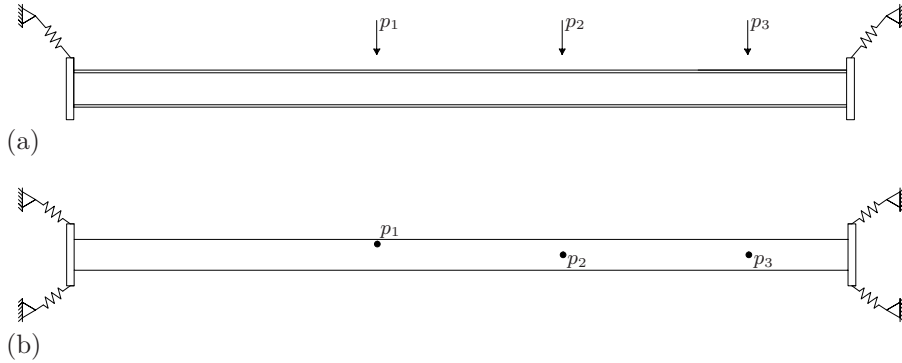


Fig. 3: Force locations as considered for Example 3.2, (a) side view and (b) top view.

Force p_1 excites the torsional modes and the bending mode, whereas forces p_2 and p_3 only excite the bending mode. The matrix $\mathbf{S}_p^T \Phi$ becomes:

$$\mathbf{S}_p^T \Phi = \begin{bmatrix} \text{T1} & \text{T2} & \text{B1} \\ * & * & * \\ 0 & 0 & * \\ 0 & 0 & * \end{bmatrix} \begin{matrix} p_1 \\ p_2 \\ p_3 \end{matrix}$$

All modes are excited by the forces and the three forces are independent. However, $\mathbf{S}_p^T \Phi$ is not of rank n_p , since the two torsional modes cannot be controlled independently by the forces assumed. As a consequence, the forces cannot be identified independently, regardless of the set of output measurements.

Example 3.3. Assume a modally reduced order model constructed from three modes of the beam, one torsional mode (mode T1) and two vertical bending modes (modes B1 and B2). Two vertical forces are acting centrally on the beam, indicated as p_1 and p_2 . The response of the structure is measured using two accelerometers. The first accelerometer, a_1 , measuring the horizontal accelerations, is placed at the web plate, right below the upper beam flange. The second accelerometer, a_2 , measuring the vertical accelerations, is placed excentrically. The force and sensor locations are shown in Fig. 4.

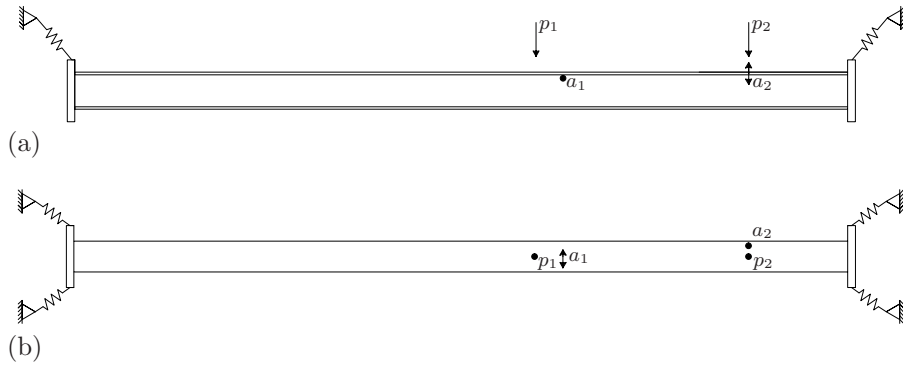


Fig. 4: Force and sensor locations as considered for Example 3.3, (a) side view and (b) top view.

Forces p_1 and p_2 excite the bending modes of the beam. The torsional mode is not excited. The matrix $\mathbf{S}_p^T \Phi$ becomes

$$\begin{bmatrix} \mathbf{S}_p^T \Phi \end{bmatrix} = \begin{bmatrix} \text{T1} & \text{B1} & \text{B2} \\ 0 & * & * \\ 0 & * & * \end{bmatrix} \begin{bmatrix} p_1 \\ p_2 \end{bmatrix}$$

Acceleration a_1 only contains a contribution from the torsional mode, whereas acceleration a_2 contains a contribution from all modes. The matrix $\mathbf{S}_{d,a} \Phi$ becomes

$$\begin{bmatrix} \mathbf{S}_{d,a} \Phi \end{bmatrix} = \begin{bmatrix} \text{T1} & \text{B1} & \text{B2} \\ * & 0 & 0 \\ * & * & * \end{bmatrix} \begin{bmatrix} a_1 \\ a_2 \end{bmatrix}$$

Both forces are independent and, in general, $\text{rank}(\mathbf{S}_p^T \Phi) = n_p$. The system will, however, not be instantaneously invertible, since there is not a direct coupling between acceleration a_1 and the excitation forces. Consequently, matrix $\mathbf{J} (= \mathbf{S}_{d,a} \Phi \Phi^T \mathbf{S}_p)$ is not of rank n_p .

4. Stability conditions

Stability of system inversion is mainly an issue for time domain inversion algorithms. The stability of the system inversion depends on the poles of the inverse system and therefore on the transmission zeros of the original system [21].

Consider the system described by Eqs. (2) and (5). A number $\lambda_j \in \mathbb{C}$ is called a finite transmission zero of the system if [26]:

$$\text{rank} \left(\begin{bmatrix} \mathbf{A} - \lambda_j \mathbf{I} & \mathbf{B} \\ \mathbf{G} & \mathbf{J} \end{bmatrix} \right) < n_s + \min(n_p, n_d) \quad (20)$$

If λ_j is a finite transmission zero of the system, there exist vectors $\mathbf{x}_{[0]} \in \mathbb{C}^{n_s}$ and $\mathbf{p}_{[0]} \in \mathbb{C}^{n_p}$ such that

$$\begin{bmatrix} \mathbf{A} - \lambda_j \mathbf{I} & \mathbf{B} \\ \mathbf{G} & \mathbf{J} \end{bmatrix} \begin{bmatrix} \mathbf{x}_{[0]} \\ \mathbf{p}_{[0]} \end{bmatrix} = \begin{bmatrix} \mathbf{0} \\ \mathbf{0} \end{bmatrix} \quad (21)$$

The input

$$\mathbf{p}_{z[k]} = \begin{cases} \mathbf{p}_{[0]} & \text{for } k = 0 \\ \mathbf{p}_{[0]} \lambda_j^k & \text{for } k = 1, 2, \dots \end{cases} \quad (22)$$

applied to the system with initial condition $\mathbf{x}_{[0]}$ then yields $\mathbf{d}_{[k]} = \mathbf{0}$ for $k = 0, 1, 2, \dots$

If a transmission zero λ_j is located inside the unit circle, i.e. $|\lambda_j| < 1$, the transmission zero is called stable. If a transmission zero is located at the unit circle, i.e. $|\lambda_j| = 1$, the transmission zero is called marginally stable. If a finite transmission zero is located outside the unit circle, i.e. $1 < |\lambda_j| < \infty$, the transmission zero is called unstable.

Theorem 4.1. *If the system described by Eqs. (2) and (5) has no finite transmission zeros, there exists an inverse system for which the poles can be arbitrarily located in the complex plane. If the system described by Eqs. (2) and (5) has no unstable or marginally stable transmission zeros, the poles of the inverse system can be chosen such that the system inversion is stable.*

Proof. The proof for continuous-time systems is given in [21] and can be readily extended to discrete-time systems. \square

Theorem 4.1 holds for instantaneous system inversion, as well as for time delayed inversion (e.g. [27]). If the system contains unstable or marginally stable zeros ($|\lambda_j| \geq 1$), a stable instantaneous inverse does not exist. By applying a time delay in the inversion process, the inverse system can be stabilized. In this paper, the focus is on instantaneous inversion, however.

The transmission zeros of a system depend on all four system matrices \mathbf{A} , \mathbf{B} , \mathbf{G} and \mathbf{J} and are found by solving the generalized eigenvalue problem given by Eq. (21). When a modally reduced order model is used, not only the mode shapes ϕ_j but also the natural frequencies ω_j and the modal damping ratios ξ_j determine the location of the system transmission zeros. In addition, the system zeros depend on the type and number of sensors used to measure the response (i.e. on the selection matrices $\mathbf{S}_{d,d}$, $\mathbf{S}_{d,v}$, and $\mathbf{S}_{d,a}$), on whether these measurements are collocated with the forces (i.e. the relation between $\mathbf{S}_{d,d}$, $\mathbf{S}_{d,v}$, $\mathbf{S}_{d,a}$ and \mathbf{S}_p), on the time discretization scheme used, etc. For these reasons, a direct relation between the output vector and the occurrence of system transmission zeros cannot be derived and the system transmission zeros have to be checked systematically for each choice of the sensor network.

Theorem 4.2. *If only acceleration and/or velocity measurements are included in the output vector, there will always be at least one purely real transmission zero $\lambda_j = 1$.*

Proof. The proof can be found in Appendix D. \square

The transmission zero $\lambda_j = 1$, located at the unit circle, corresponds to excitation at a frequency of 0 Hz (see Eq. (22), $\mathbf{p}_z[k] = \mathbf{p}_{[0]}$ for all k if $\lambda_j = 1$). The zero occurs because both acceleration and velocity measurements are insensitive to excitation which is constant in time. If no unstable system zeros are present, the instantaneous inversion will be marginally stable. This is commonly encountered in structural dynamics, where acceleration measurements are used extensively, as they can be accurately measured at a relatively low cost.

Theorem 4.3. *Transmission zeros of the system corresponding to a frequency of 0 Hz can be avoided by requiring that $\text{rank}(\mathbf{J} - \mathbf{G}(\mathbf{A} - \mathbf{I})^{-1}\mathbf{B}) = \min(n_p, n_d)$.*

Proof. The proof can be found in Appendix E. □

Proposition 4.1. *The matrix $\mathbf{J} - \mathbf{G}(\mathbf{A} - \mathbf{I})^{-1}\mathbf{B}$ is of rank $\min(n_p, n_d)$ only if the number of displacement/strain measurements $n_{d,d}$ is larger than or equal to the number of forces n_p .*

Proof. The proof can be found in Appendix F. □

Imposing that $\text{rank}(\mathbf{J} - \mathbf{G}(\mathbf{A} - \mathbf{I})^{-1}\mathbf{B}) = \min(n_p, n_d)$ ensures a direct coupling between the measured displacement/strain responses and the estimated forces through at least n_p modes composing the model. The choice of displacement or strain measurements (number of measurements, measurement locations and directions) is based on the same principles as the choice of acceleration measurements, needed for system invertibility (section 3.3). The reader is referred to Example 3.3 for an illustration of the concept.

5. Uniqueness conditions

The uniqueness of the identified forces and/or system states depends on the system transmission zeros, as stated in the following corollary:

Corollary 5.1. *The input of a system with at least one finite transmission zero cannot be uniquely reconstructed.*

This follows directly from the definition of a system transmission zero: there exists an input and an initial state for which the system output is zero (Eq. (21)). As a consequence, the input cannot be uniquely reconstructed from the measured output. When the forces and system states are jointly estimated, both estimated quantities cannot be uniquely determined.

Example 5.1. When the system output only consists of acceleration measurements, the static component of both the identified forces and system states cannot be retrieved from the measurements. By adding displacement and/or strain measurements, such that $\text{rank}(\mathbf{J} - \mathbf{G}(\mathbf{A} - \mathbf{I})^{-1}\mathbf{B}) = \min(n_p, n_d)$, the static component is identified as well.

6. Implementation for a footbridge model

In this section, the conditions as derived above are implemented in the design of a sensor network for a footbridge that allows for the identification of multiple forces on the bridge deck. The footbridge, depicted in Fig. 5, is located in Ninove (Belgium) where it crosses the Dender river. It is a two-span cable-stayed steel bridge with a main and secondary span of 36 m and 22.5 m, respectively.



Fig. 5: The footbridge in Ninove, Belgium.

6.1. System model

The system matrices are constructed from a finite element (FE) model of the bridge, developed using the FE program ANSYS. The model has been calibrated using a set of experimentally identified modal characteristics, which are obtained through a combined output-only [28] and input-output system identification procedure [23]. The first 3 modes calculated using the calibrated FE model are shown in Fig. 6.

A reduced-order discrete-time state-space model is constructed from the FE model of the footbridge, applying a zero order hold assumption on the force. The model includes the 15 modes listed in Table 1. For each mode, the mass normalized mode shape is assumed to be known from the FE model, whereas the natural frequency and the modal damping ratio are taken as the experimentally identified values. Table 1 presents the experimentally identified modal characteristics. The system model is now used to illustrate the design of a sensor network for input estimation, hereby implementing the conditions as outlined in the first part of this paper.

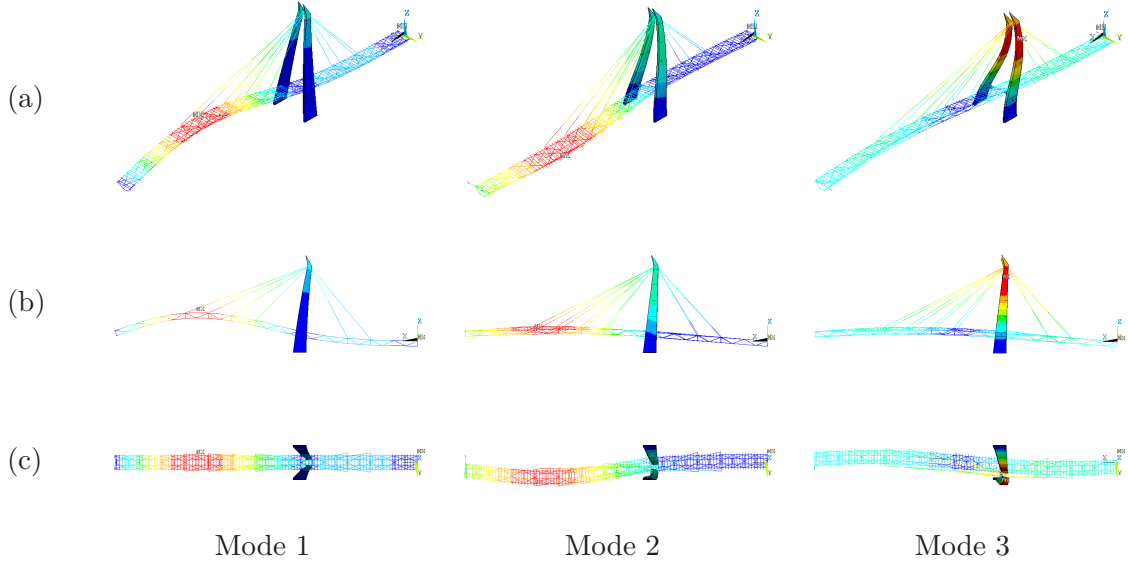


Fig. 6: Results of the FE modal analysis for the first 3 modes (displacement vector sum) (a) 3D-view, (b) front view and (c) top view. Modes correspond to the calibrated FE model.

No.	f_{id} [Hz]	ξ_{id} [%]	$\omega_{id,d}$ [rad s ⁻¹]	Description
1	2.98	0.40	18.72	First vertical bending main span
2	3.08	0.67	19.35	First lateral bending main span
3	3.81	0.58	23.94	First lateral bending main and secondary span
4	5.84	0.89	36.69	First lateral bending secondary span
5	6.00	0.67	37.70	First vertical bending secondary span
6	6.92	0.29	43.48	First torsion main span
7	8.00	0.76	50.26	Second vertical bending main span
8	9.84	0.48	61.83	Second lateral bending main and secondary span
9	10.98	0.87	68.99	First torsion secondary span
10	12.52	1.62	78.66	Third lateral bending main and secondary span
11	13.55	0.52	85.14	Third vertical bending main span
12	14.02	0.16	88.09	Third lateral bending main span
13	14.71	0.57	92.42	Second vertical bending secondary span
14	17.29	0.14	108.64	Fourth lateral bending main span
15	18.57	0.46	116.68	Fourth vertical bending main span

Table 1: Experimentally identified modal characteristics (f_{id} : natural frequency, ξ_{id} : modal damping ratio, and $\omega_{id,d}$: damped natural frequency).

6.2. Design of sensor network

Consider two forces to be estimated (i.e. pure input estimation). The forces are applied vertically to the bridge deck, at node 27 and node 48 (see Fig. 7). The locations and directions of the forces are assumed known. A set of five possible sensor locations is indicated in Fig 7. For each of these locations, the vertical (z-direction) and lateral (y-direction) response can be measured (displacement, velocity or acceleration). The total number of candidate measurement locations is limited to five for this theoretical example, but can be readily extended.

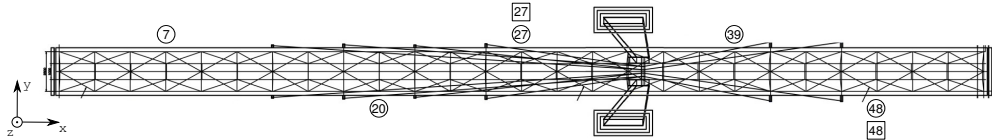


Fig. 7: Overview of the force locations (squares) and possible sensor locations (circles).

The forces are denoted by p_{27z} and p_{48z} . Response measurements are denoted by $\alpha i \zeta$, where α refers to the sensor type (a : acceleration, v : velocity, d : displacement), i refers to the number of the measurement location (node number) and ζ denotes the measurement direction (z or y).

The design of the sensor network now consists of determining a subset of output measurements such that the estimation of the applied forces becomes possible. Since force identification is aimed at, the system states as such are not of interest, and observability is not required. In addition, the force locations and directions are known and, therefore, system controllability is not relevant for this case. The direct invertibility conditions, the stability conditions, and the uniqueness conditions are implemented in the following paragraphs.

6.2.1. Direct invertibility conditions

Direct invertibility requires the direct transmission matrix \mathbf{J} to be of rank n_p (Theorem 3.5). In order to check if $\text{rank}(\mathbf{S}_p^T \Phi) = n_p$ (Proposition 3.3), one could first verify whether for each subset

of $n_{p,e}$ forces (with $n_{p,e} \leq n_p$) the number of modes excited $n_{m,e}$ is larger than or equal to $n_{p,e}$, and check the rank of $\mathbf{S}_p^T \Phi$ hereafter. The number of modes excited by a subset of $n_{p,e}$ forces is found as the number of non-zero columns of the matrix $\mathbf{S}_{p,e}^T \Phi$, where $\mathbf{S}_{p,e} \in \mathbb{R}^{n_{\text{dof}} \times n_{p,e}}$ is obtained from the matrix \mathbf{S}_p by retaining the columns corresponding to the subset of $n_{p,e}$ forces.

Fig. 8 shows a graphical representation of the matrix $\mathbf{S}_p^T \Phi$, indicating the modes (columns) excited by the forces (rows). For this case study, the two forces to be estimated are independent and excite a large number of modes (≥ 2), as seen from Fig. 8. Therefore, $\mathbf{S}_p^T \Phi$, will be of full rank. As a verification, the singular values of the matrix $\mathbf{S}_p^T \Phi$ are shown in Fig. 11a. The two singular values are larger than zero and the rank of $\mathbf{S}_p^T \Phi$ equals two. If this were not the case, it would not be possible to identify the two forces independently, regardless of the set of output measurements (Proposition 3.3).

Imposing that $\mathbf{S}_p^T \Phi$ must be of rank n_p is necessary but not sufficient for guaranteeing that \mathbf{J} is of rank n_p . In addition, at least n_p acceleration measurements are required (Proposition 3.4), that ensure a direct coupling between the measured acceleration responses and the estimated forces through at least n_p modes composing the model. In order to check if $\text{rank}(\mathbf{J}) = n_p$, one could first verify whether for each subset of $n_{p,e}$ forces the modes excited ($n_{m,e}$ modes) contribute to at least $n_{p,e}$ acceleration responses, and calculate the rank of \mathbf{J} hereafter. The modes excited by a subset of $n_{p,e}$ forces are found from the non-zero columns of the matrix $\mathbf{S}_{p,e}^T \Phi$. The number of acceleration responses containing a contribution from a subset of $n_{m,e}$ modes is found as the number of non-zero rows of the matrix $\mathbf{S}_{d,a} \Phi_e$, where $\Phi_e \in \mathbb{R}^{n_{\text{dof}} \times n_{m,e}}$ is obtained from the matrix Φ by retaining the columns corresponding to the subset of the $n_{m,e}$ modes excited.

Fig. 9 shows a graphical representation of the matrix $\mathbf{S}_{d,\alpha} \Phi$, indicating the contribution of the modes (columns) to each of the possible outputs (rows). At this point, no distinction is made between displacement, velocity, and acceleration measurements. The matrix $\mathbf{S}_d \Phi$ corresponding to the true sensor layout will thus be a combination of rows of the matrix $\mathbf{S}_{d,\alpha} \Phi$, shown in Fig. 9. For this case study, at least two acceleration measurements are required. By selecting two collocated acceleration measurements, i.e. **da27z** and **da48z**, the input-output coupling is assured in this case and the matrix \mathbf{J} is of rank n_p . If, however, it is not possible to perform collocated measurements, the acceleration measurements are preferably chosen such that the coupling through the modes significantly excited by the forces, is large.

A choice can be made based on the graphical representation of the matrices $\mathbf{S}_p^T \Phi$ and $\mathbf{S}_{d,\alpha} \Phi$, shown in Fig. 8 and Fig. 9, respectively. The coupling between a force **pjz** and a single output **daiζ** is studied by comparing the corresponding row of the matrices $\mathbf{S}_p^T \Phi$ and $\mathbf{S}_{d,\alpha} \Phi$, respectively. An appropriate set of non-collocated acceleration measurements in this case consists of the vertical accelerations **da7z** and **da39z**. For the force at node 27 (**p27z**), there is a strong coupling to the output **da7z** through modes 7, 11, and 15. For the force at node 48 (**p48z**), there is a strong coupling to the output **da39z** through modes 5, 9, and 13. For the set of two non-collocated acceleration measurements, **da7z** and **da39z**, the singular values of the matrix \mathbf{J} are shown in Fig. 11b. As all singular values are larger than zero, the rank of \mathbf{J} equals two.

For the remainder of this example, the two acceleration measurements **da7z** and **da39z** are included in the data vector $\mathbf{d}_{[k]}$. This set of measurements can, however, be extended taking into account the remaining requirements on stability and uniqueness.

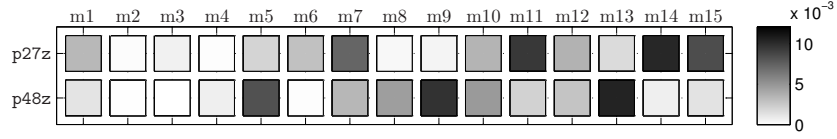


Fig. 8: Graphical representation of the matrix $\mathbf{S}_p^T \Phi$. Absolute value of the matrix elements is shown.

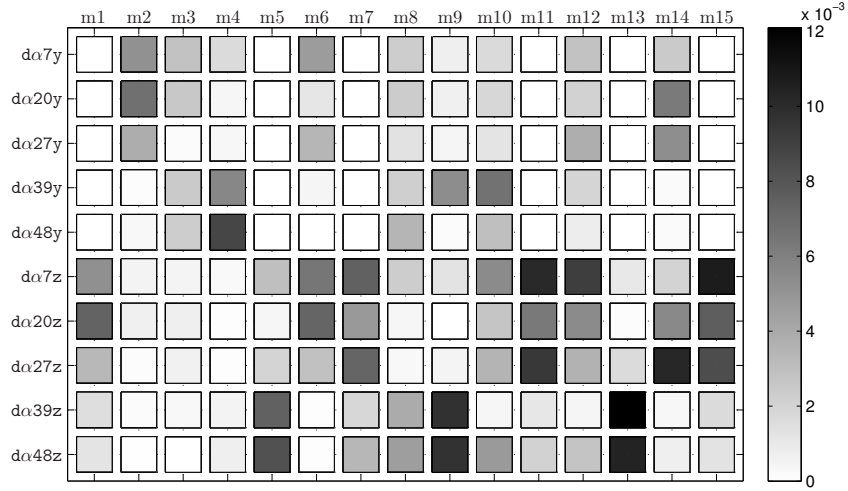


Fig. 9: Graphical representation of the matrix $\mathbf{S}_{d,\alpha} \Phi$ used in the design of the sensor network. Absolute value of the matrix elements is shown.

6.2.2. Stability conditions

Starting from the set of acceleration measurements selected in section 6.2.1, i.e. **da7z** and **da39z**, it is now investigated how the set of output measurements has to be extended, in order to ensure the stability of the system inversion algorithm.

Figure 10 shows the finite transmission zeros for the system with input **p27z**, **p48z**, and output **da7z**, **da39z** (2 acceleration measurements). From the figure, it is clear that some zeros are unstable. Therefore, stable instantaneous system inversion will not be possible.

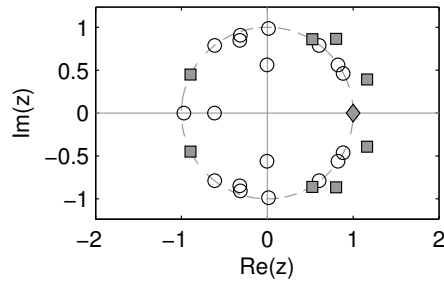


Fig. 10: System transmission zeros in the z -plane (input: **p27z** and **p48z**, output: **da7z** and **da39z**). Stable transmission zeros are indicated by circles, unstable zeros by solid squares, and marginally stable zeros by solid diamonds.

In order to obtain a system with only stable finite transmission zeros, additional outputs have to be included in the output vector $\mathbf{d}_{[k]}$. Since displacement (or strain) measurements are required in any case to avoid marginally stable zeros, corresponding to a transmission zero frequency of 0 Hz (indicated by solid diamond in Fig. 10), additional displacement measurements are defined

first.

At least n_p displacement/strain measurements are required (Proposition 4.1), that ensure a direct coupling between the measured displacement/strain responses and the estimated forces through at least n_p modes composing the model. In order to check if $\text{rank}(\mathbf{J} - \mathbf{G}(\mathbf{A} - \mathbf{I})^{-1}\mathbf{B}) = \min(n_p, n_d)$, one could first verify whether for each subset of $n_{p,e}$ forces the modes excited ($n_{m,e}$ modes) contribute to at least $n_{p,e}$ displacement or strain responses, and calculate the rank of $\mathbf{J} - \mathbf{G}(\mathbf{A} - \mathbf{I})^{-1}\mathbf{B}$ hereafter. The modes excited by a subset of $n_{p,e}$ forces are found from the non-zero columns of the matrix $\mathbf{S}_{p,e}^T \Phi$, where $\mathbf{S}_{p,e} \in \mathbb{R}^{n_{\text{dof}} \times n_{p,e}}$ is obtained from the matrix \mathbf{S}_p by retaining the columns corresponding to the subset of $n_{p,e}$ forces. The number of displacement/strain responses containing a contribution from a subset of $n_{m,e}$ modes is found as the number of non-zero rows of the matrix $\mathbf{S}_{d,e} \Phi_e$, where $\Phi_e \in \mathbb{R}^{n_{\text{dof}} \times n_{m,e}}$ is obtained from the matrix Φ by retaining the columns corresponding to the subset of the $n_{m,e}$ modes excited.

For this case study, at least two displacement measurements are required in order to avoid marginally stable zeros. The selection of two collocated displacement measurements is recommended to ensure input-output coupling, i.e. **dd27z** and **dd48z**, but other choices can be made, based on Fig. 8 and Fig. 9. One possible non-collocated choice here is to extend the set of acceleration measurements by two displacement measurements, chosen as **dd20z** and **dd39y**. For the force at node 27 (**p27z**), there is a coupling to the output **dd20z** through a large number of modes. For the force at node 48 (**p48z**), there is a coupling to the output **dd39y**, particularly through modes 9 and 10. For the set of output measurements **da7z**, **da39z**, **dd20z**, and **dd39y**, the singular values of the matrix $\mathbf{J} - \mathbf{G}(\mathbf{A} - \mathbf{I})^{-1}\mathbf{B}$ are shown in Fig. 11c. As all singular values are larger than zero, the matrix is of rank two. The system obtained by adding the two displacement measurements to the output vector does no longer have finite transmission zeros and stable inversion of the system is possible.

6.2.3. Uniqueness conditions

In section 6.2.2, it is mentioned that for the set of output measurements **da7z**, **da39z**, **dd20z**, and **dd39y**, the system does not have finite transmission zeros. Therefore, the input of the system can be uniquely reconstructed from the measured output. The uniqueness condition in this case does not impose additional constraints.

The measurement setup as retained is summarized in Table 2. For the selection, it is assumed that collocated measurements cannot be performed.

No.	Code	Node	Type	Direction	Main reason for selection
1	da7z	7	Acceleration	Vertical	Direct invertibility (section 6.2.1)
2	da39z	39	Acceleration	Vertical	Direct invertibility (section 6.2.1)
3	dd20z	20	Displacement	Vertical	Stability conditions (section 6.2.2)
4	dd39y	39	Displacement	Lateral	Stability conditions (section 6.2.2)

Table 2: Summary of the output measurements selected taking into account the general conditions for instantaneous system inversion.

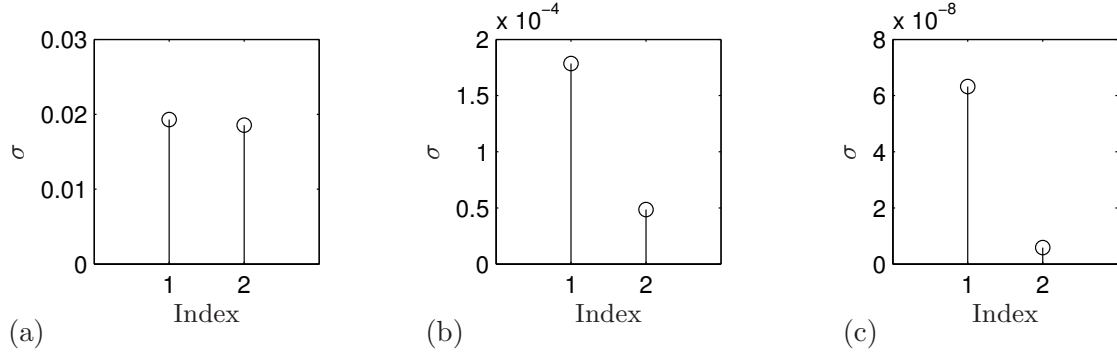


Fig. 11: Singular values of (a) matrix $\mathbf{S}_p^T \Phi$, (b) matrix \mathbf{J} ($= \mathbf{S}_{d,a} \Phi \Phi^T \mathbf{S}_p$, output: `da7z` and `da39z`), and (c) matrix $\mathbf{J} - \mathbf{G}(\mathbf{A} - \mathbf{I})^{-1} \mathbf{B}$ (output: `da7z`, `da39z`, `dd20z`, and `dd39y`).

7. Conclusions

In this paper, general conditions for the invertibility of linear system models have been presented for the specific case of modally reduced order models. The conditions apply to any instantaneous input estimation or joint input-state estimation algorithm and ensure the identifiability, stability, and uniqueness of the identified quantities. It is shown that the general invertibility conditions can be reformulated in terms of the modal characteristics of the structure. The practical implementation of the invertibility conditions is discussed for a case study where a sensor network for a footbridge is designed.

Acknowledgments

The research presented in this paper has been performed within the framework of the project G.0738.11 “Inverse identification of wind loads on structures”, funded by the Research Foundation Flanders (FWO), Belgium. Their financial support is gratefully acknowledged. The authors are all members of the KU Leuven - BOF PFV/10/002 OPTEC - Optimization in Engineering Center. E. Reynders is a Postdoctoral Fellow of the Research Foundation Flanders (FWO), Flanders.

References

- [1] P. Guillaume, E. Parloo, G. De Sitter, Source identification from noisy response measurements using an iterative weighted pseudo-inverse approach., in: *Proceedings of ISMA2002 International Conference on Noise and Vibration Engineering*, Leuven, Belgium, pp. 1817–1824.
- [2] Y. Liu, W. Shepard, Dynamic force identification based on enhanced least squares and total least squares schemes in the frequency domain, *Journal of Sound and Vibration* 282 (2005) 37–60.
- [3] E. Parloo, P. Verboven, P. Guillaume, M. Van Overmeire, Force identification by means of in-operational modal models, *Journal of Sound and Vibration* 262 (2003) 161–173.
- [4] M. Klinkov, C.-P. Fritzen, An updated comparison of the force reconstruction methods, *Key Engineering Materials* 347 (2007) 461–466.
- [5] L. Nordström, T. Nordberg, A critical comparison of time domain load identification methods, in: *Proceedings of the 6th International Conference on Motion and Vibration Control*, Saitama, Japan, pp. 1151–1156.
- [6] E. Jacquelin, A. Bannani, P. Hamelin, Force reconstruction: analysis and regularization of a deconvolution problem, *Journal of Sound and Vibration* 265 (2003) 81–107.
- [7] R. Adams, J. Doyle, Multiple force identification for complex structures, *Experimental Mechanics* 42 (2002) 25–36.
- [8] J. Ching, J. Beck, K. Porter, Bayesian state and parameter estimation of uncertain dynamical systems, *Probabilistic Engineering Mechanics* 21 (2006) 81–96.
- [9] M. Wu, A. Smyth, Application of the unscented Kalman filter for real-time nonlinear structural system identification, *Structural Control and Health Monitoring* 14 (2007) 971–990.
- [10] E. Hernandez, D. Bernal, State estimation in structural systems with model uncertainties, *ASCE Journal of Engineering Mechanics* 134 (2008) 252–257.
- [11] E. Hernandez, A natural observer for optimal state estimation in second order linear structural systems, *Mechanical Systems and Signal Processing* 25 (2011) 2938–2947.
- [12] M. Klinkov, C.-P. Fritzen, Online estimation of external loads from dynamic measurements, in: P. Sas, M. D. Munck (Eds.), *Proceedings ISMA2006*, Leuven, Belgium, pp. 3957–3968.
- [13] J. Hwang, A. Kareem, W. Kim, Estimation of modal loads using structural response, *Journal of Sound and Vibration* 326 (2009) 522–539.
- [14] C. Ma, J. Chang, D. Lin, Input forces estimation of beam structures by an inverse method, *Journal of Sound and Vibration* 259 (2003) 387–407.
- [15] S. Gillijns, B. De Moor, Unbiased minimum-variance input and state estimation for linear discrete-time systems with direct feedthrough, *Automatica* 43 (2007) 934–937.
- [16] E. Lourens, C. Papadimitriou, S. Gillijns, E. Reynders, G. De Roeck, G. Lombaert, Joint input-response estimation for structural systems based on reduced-order models and vibration data from a limited number of sensors, *Mechanical Systems and Signal Processing* 29 (2012) 310–327.
- [17] Y. Niu, M. Klinkov, C.-P. Fritzen, Online force reconstruction using an unknown-input Kalman filter approach., in: *Proceedings of the 8th International Conference on Structural Dynamics*, EUROODYN 2011, Leuven, Belgium, pp. 2569–2576.
- [18] E. Lourens, E. Reynders, G. De Roeck, G. Degrande, G. Lombaert, An augmented Kalman filter for force identification in structural dynamics, *Mechanical Systems and Signal Processing* 27 (2012) 446–460.
- [19] P. Antsaklis, Stable proper n th-order inverses, *IEEE Transactions on Automatic Control* 23 (1978) 1104–1106.
- [20] J. Massey, M. Sain, Inverses of linear sequential circuits, *IEEE Transactions on Automatic Control* 17 (1968) 330–337.
- [21] P. Moylan, Stable inversion of linear systems, *IEEE Transactions on Automatic Control* 22 (1977) 74–78.
- [22] G. Franklin, J. Powell, M. Workman, *Digital control of dynamic systems*, Addison-Wesley, Menlo Park, CA, third edition, 1998.
- [23] E. Reynders, G. De Roeck, Reference-based combined deterministic-stochastic subspace identification for experimental and operational modal analysis, *Mechanical Systems and Signal Processing* 22 (2008) 617–637.
- [24] T. Glad, L. Ljung, *Control Theory: Multivariable and Nonlinear Methods*, Taylor & Francis, New York, USA, first edition, 2000.
- [25] D. Bernstein, *Matrix Mathematics: Theory, Facts, and Formulas with Application to Linear Systems Theory*, Princeton University Press, Princeton, New Jersey, second edition, 2009.
- [26] T. Kailath, *Linear systems*, Prentice-Hall, Englewood Cliffs, N.J., 1980.
- [27] C. Hsieh, Optimal time-delayed joint input and state estimation for systems with unknown inputs, in: *Proceedings of the 48th IEEE Conference on Decision and Control*, Shanghai.

- [28] B. Peeters, G. De Roeck, Reference-based stochastic subspace identification for output-only modal analysis, *Mechanical Systems and Signal Processing* 13 (1999) 855–878.
- [29] E. Reynders, System identification methods for (operational) modal analysis: review and comparison, *Archives of Computational Methods in Engineering* 19 (2012) 51–124.
- [30] G. Franklin, J. Powell, A. Emami-Naeini, *Feedback Control of Dynamic Systems*, Pearson Education, 2011.

Appendix A. Decoupling of a state-space model

Consider a transformation of the state vector $\mathbf{x}_{[k]} \rightarrow \mathbf{T}^{-1}\mathbf{x}_{[k]}$, with $\mathbf{T} \in \mathbb{C}^{n_s \times n_s}$ a nonsingular matrix. A transformation of the system matrices $(\mathbf{A}, \mathbf{B}, \mathbf{G}, \mathbf{J}) \rightarrow (\mathbf{T}^{-1}\mathbf{A}\mathbf{T}, \mathbf{T}^{-1}\mathbf{B}, \mathbf{G}\mathbf{T}, \mathbf{J})$ preserves the input-output map provided by the state-space description and corresponds to the transformation of the state vector under \mathbf{T}^{-1} .

The system defined by Eqs. (2) and (5) is decoupled by putting $\mathbf{T} = \mathbf{\Psi}_d$, with $\mathbf{\Psi}_d \in \mathbb{C}^{n_s \times n_s}$ a matrix containing the eigenvectors of \mathbf{A} as columns [29]:

$$\mathbf{A}\mathbf{\Psi}_d = \mathbf{\Psi}_d\mathbf{\Lambda}_d \quad (\text{A.1})$$

where $\mathbf{\Lambda}_d \in \mathbb{C}^{n_s \times n_s}$ is a diagonal matrix containing the damped eigenvalues $\lambda_{d,n}$ of \mathbf{A} on its diagonal. The system obtained after transformation is given by:

$$\mathbf{x}_{m[k+1]} = \mathbf{\Lambda}_d\mathbf{x}_{m[k]} + \mathbf{L}_d^T\mathbf{p}_{[k]} \quad (\text{A.2})$$

$$\mathbf{d}_{[k]} = \mathbf{\Phi}_d\mathbf{x}_{m[k]} + \mathbf{J}\mathbf{p}_{[k]} \quad (\text{A.3})$$

The state-output matrix of the decoupled system $\mathbf{\Phi}_d$ is given by:

$$\mathbf{\Phi}_d = [\mathbf{\Phi}_{ds} \quad \overline{\mathbf{\Phi}_{ds}}] \quad (\text{A.4})$$

where, as shown in [29]:

$$\mathbf{\Phi}_{ds} = \mathbf{S}_{d,d}\mathbf{\Phi} + i\mathbf{S}_{d,v}\mathbf{\Phi}\mathbf{\Omega}_d - \mathbf{S}_{d,a}\mathbf{\Phi}\mathbf{\Omega}_d^2 \quad (\text{A.5})$$

In the equation above, $\mathbf{\Omega}_d \in \mathbb{C}^{n_m \times n_m}$ is a diagonal matrix containing the damped natural frequencies $\omega_{d,j}$ on its diagonal, where $\omega_{d,j} = \omega_j\sqrt{1 - \xi_j^2}$ for proportionally damped structures, which is related to $\lambda_{d,n}$ in Eq. (A.1) as: $\lambda_{d,n} = e^{i\omega_{d,n}\Delta t}$ if $n \leq n_m$, and $\lambda_{d,n} = e^{-i\omega_{d,n-n_m}\Delta t}$ if $n > n_m$, with Δt the sampling time step. The overbar in Eq. (A.4) denotes the complex conjugate of a matrix. It is assumed that the eigenvectors of \mathbf{A} , i.e. the columns of the matrix $\mathbf{\Psi}_d$, are ordered and scaled such that Eqs. (A.4) and (A.5) hold, given that the mode shapes $\mathbf{\Phi}$ are scaled to unit modal mass. The proof, however, can be readily extended to the general case where the columns of $\mathbf{\Psi}_d$ are arbitrarily scaled.

The state-input matrix of the decoupled system \mathbf{L}_d^T in Eq. (A.2) is given by:

$$\mathbf{L}_d^T = [\mathbf{L}_{ds} \quad \overline{\mathbf{L}_{ds}}]^T \quad (\text{A.6})$$

\mathbf{L}_{ds} is a matrix containing the modal participation factors as columns. In accordance to the dynamic (Betti-Rayleigh) reciprocity theorem, it is found that:

$$\mathbf{L}_{ds} = \mathbf{S}_p^T\mathbf{\Phi}\mathbf{Q}_s \quad (\text{A.7})$$

where $\mathbf{Q}_s \in \mathbb{C}^{n_m \times n_m}$ is a nonsingular diagonal matrix containing the modal scaling factors q_j on its diagonal [29].

Appendix B. Proof of Theorem 3.2

A transformation of the state vector $\mathbf{x}_{[k]} \rightarrow \mathbf{T}^{-1}\mathbf{x}_{[k]}$ and the corresponding transformation of the system, as considered in Appendix A, do not affect the system observability. This is shown next.

The observability matrix \mathcal{O}' of the system obtained after transformation is given by:

$$\mathcal{O}' = \begin{bmatrix} \mathbf{GT} \\ \mathbf{GAT} \\ \vdots \\ \mathbf{GA}^{n_s-1}\mathbf{T} \end{bmatrix} = \mathcal{O}\mathbf{T} \quad (\text{B.1})$$

with \mathcal{O} the observability matrix of the original system, as defined in Eq. (9). Since the matrix \mathbf{T} is of full rank, the rank of \mathcal{O} equals the rank of \mathcal{O}' [25].

For $\mathbf{T} = \mathbf{\Psi}_d$, with $\mathbf{\Psi}_d$ the matrix containing the eigenvectors of \mathbf{A} (see Eq. (A.1)), the decoupled system given by Eqs. (A.2) and (A.3) is obtained. The observability matrix of the decoupled system is given by:

$$\mathcal{O}' = \begin{bmatrix} \mathbf{G}\mathbf{\Psi}_d \\ \mathbf{GA}\mathbf{\Psi}_d \\ \vdots \\ \mathbf{GA}^{2n_m-1}\mathbf{\Psi}_d \end{bmatrix} = \begin{bmatrix} \mathbf{\Phi}_d \\ \mathbf{\Phi}_d\mathbf{\Lambda}_d \\ \vdots \\ \mathbf{\Phi}_d\mathbf{\Lambda}_d^{2n_m-1} \end{bmatrix} \quad (\text{B.2})$$

By applying elementary row operations it can be shown that \mathcal{O}' is row equivalent to the following matrix:

$$\mathcal{O}'' = \begin{bmatrix} \phi_{d,1} & \phi_{d,2} & \cdots & \phi_{d,2n_m} \\ \mathbf{0} & \phi_{d,2}(\lambda_{d,2} - \lambda_{d,1}) & \cdots & \phi_{d,2n_m}(\lambda_{d,2n_m} - \lambda_{d,1}) \\ \vdots & \vdots & \ddots & \vdots \\ \mathbf{0} & \mathbf{0} & \cdots & \phi_{d,2n_m} \prod_{n=1}^{2n_m-1} (\lambda_{d,2n_m} - \lambda_{d,n}) \end{bmatrix} \quad (\text{B.3})$$

where $\phi_{d,n} \in \mathbb{C}^{n_d}$ is the n -th column of the matrix $\mathbf{\Phi}_d$. The rank of \mathcal{O}'' equals the rank of \mathcal{O}' and thus of \mathcal{O} . Therefore, \mathcal{O} is of full rank if and only if for all eigenvalues, with each eigenvalue having multiplicity m_k (i.e. $\lambda_{d,n} = \lambda_{d,n+1} = \dots = \lambda_{d,n+m_k-1}$), the following equation holds:

$$\text{rank}([\phi_{d,n} \quad \phi_{d,n+1} \quad \cdots \quad \phi_{d,n+m_k-1}]) = m_k \quad (\text{B.4})$$

where $1 \leq m_k \leq n_m$ for damped structures. From Eqs. (A.4) and (A.5) it follows that Eq. (B.4) holds if and only if for all damped natural frequencies, with each damped natural frequency having multiplicity m_l (i.e. $\omega_{d,j} = \omega_{d,j+1} = \dots = \omega_{d,j+m_l-1}$), the following equation holds:

$$\text{rank}((\mathbf{S}_{d,d} + i\omega_{d,j}\mathbf{S}_{d,v} - \omega_{d,j}^2\mathbf{S}_{d,a})[\phi_j \quad \phi_{j+1} \quad \cdots \quad \phi_{j+m_l-1}]) = m_l \quad (\text{B.5})$$

where ϕ_j is the mass-normalized mode shape of mode j , and $\omega_{d,j} = \omega_j \sqrt{1 - \xi_j^2}$ is the damped natural frequency corresponding to mode j , with $j = n$ if $n \leq n_m$ and $j = n - n_m$ if $n > n_m$, n_m is the number of modes taken into account in the model. Under the assumption that each element of the output vector $\mathbf{d}(t)$ consists of either an acceleration measurement, a velocity measurement, a

displacement measurement or a strain measurement, i.e. every non-zero row in one of the selection matrices $\mathbf{S}_{d,a}$, $\mathbf{S}_{d,v}$ and $\mathbf{S}_{d,d}$ corresponds to a zero row in the other two matrices, and for $\omega_{d,j} \neq 0$, Eq. (B.5) is equivalent to Eq. (B.6):

$$\text{rank}((\mathbf{S}_{d,d} + \mathbf{S}_{d,v} + \mathbf{S}_{d,a})[\phi_j \quad \phi_{j+1} \quad \dots \quad \phi_{j+m_l-1}]) = m_l \quad (\text{B.6})$$

The matrix $(\mathbf{S}_{d,d} + \mathbf{S}_{d,v} + \mathbf{S}_{d,a})[\phi_j \quad \phi_{j+1} \quad \dots \quad \phi_{j+m_l-1}]$ in Eq. (B.6) is obtained from the matrix $(\mathbf{S}_{d,d} + i\omega_{d,j}\mathbf{S}_{d,v} - \omega_{d,j}^2\mathbf{S}_{d,a})[\phi_j \quad \phi_{j+1} \quad \dots \quad \phi_{j+m_l-1}]$ in Eq. (B.5) by multiplying each row by a non-zero scaling factor. These row operations do not affect the matrix rank [25].

Appendix C. Proof of Theorem 3.4

A transformation of the state vector $\mathbf{x}_{[k]} \rightarrow \mathbf{T}^{-1}\mathbf{x}_{[k]}$ and the corresponding transformation of the system, as considered in Appendix B, do not affect the system controllability. This is shown next.

The controllability matrix \mathbf{C}' of the system obtained after transformation is given by:

$$\mathbf{C}' = [\mathbf{T}^{-1}\mathbf{B} \quad \mathbf{T}^{-1}\mathbf{A}\mathbf{B} \quad \dots \quad \mathbf{T}^{-1}\mathbf{A}^{n_s-1}\mathbf{B}] = \mathbf{T}^{-1}\mathbf{C} \quad (\text{C.1})$$

with \mathbf{C} the controllability matrix of the original system, as defined in Eq. (13). Since the matrix \mathbf{T}^{-1} is of full rank, the rank of \mathbf{C} equals the rank of \mathbf{C}' [25].

For $\mathbf{T} = \mathbf{\Psi}_d$, with $\mathbf{\Psi}_d$ the matrix containing the eigenvectors of \mathbf{A} (see Eq. (A.1)), the decoupled system given by Eqs. (A.2) and (A.3) is obtained. The controllability matrix of the decoupled system is given by:

$$\mathbf{C}' = [\mathbf{\Psi}_d^{-1}\mathbf{B} \quad \mathbf{\Psi}_d^{-1}\mathbf{A}\mathbf{B} \quad \dots \quad \mathbf{\Psi}_d^{-1}\mathbf{A}^{2n_m-1}\mathbf{B}] = [\mathbf{L}_d^T \quad \mathbf{\Lambda}_d\mathbf{L}_d^T \quad \dots \quad \mathbf{\Lambda}_d^{2n_m-1}\mathbf{L}_d^T] \quad (\text{C.2})$$

By applying elementary column operations it can be shown that \mathbf{C}' is column equivalent to the following matrix:

$$\mathbf{C}'' = \begin{bmatrix} \mathbf{l}_{d,1}^T & \mathbf{0} & \dots & \mathbf{0} \\ \mathbf{l}_{d,2}^T & \mathbf{l}_{d,2}^T(\lambda_{d,2} - \lambda_{d,1}) & \dots & \mathbf{0} \\ \vdots & \vdots & \ddots & \vdots \\ \mathbf{l}_{d,2n_m}^T & \mathbf{l}_{d,2n_m}^T(\lambda_{d,2n_m} - \lambda_{d,1}) & \dots & \mathbf{l}_{d,2n_m}^T \prod_{n=1}^{2n_m-1} (\lambda_{d,2n_m} - \lambda_{d,n}) \end{bmatrix} \quad (\text{C.3})$$

where $\mathbf{l}_{d,n}$ is the n -th column of the matrix \mathbf{L}_d . The rank of \mathbf{C}'' equals the rank of \mathbf{C}' and thus of \mathbf{C} . Therefore, \mathbf{C} is of full rank if and only if for all eigenvalues, with each eigenvalue having multiplicity m_k (i.e. $\lambda_{d,n} = \lambda_{d,n+1} = \dots = \lambda_{d,n+m_k-1}$), the following equation holds:

$$\text{rank}([\mathbf{l}_{d,n} \quad \mathbf{l}_{d,n+1} \quad \dots \quad \mathbf{l}_{d,n+m_k-1}]) = m_k \quad (\text{C.4})$$

where $1 \leq m_k \leq n_m$ for damped structures. From Eqs. (A.6) and (A.7) it follows that Eq. (C.4) holds if and only if for all damped natural frequencies, with each damped natural frequency having multiplicity m_l (i.e. $\omega_{d,j} = \omega_{d,j+1} = \dots = \omega_{d,j+m_l-1}$), the following equation holds:

$$\text{rank}(\mathbf{S}_p^T[q_j\phi_j \quad q_{j+1}\phi_{j+1} \quad \dots \quad q_{j+m_l-1}\phi_{j+m_l-1}]) = m_l \quad (\text{C.5})$$

where ϕ_j is the mass-normalized mode shape of mode j , and q_j is the modal scaling factor of mode j , i.e. the j -th diagonal element of the matrix \mathbf{Q}_s in Eq. (A.7), with $j = n$ if $n \leq n_m$, and

$j = n - n_m$ if $n > n_m$, n_m is the number of modes taken into account in the model. For $q_j \neq 0$, Eq. (C.5) is equivalent to Eq. (C.6):

$$\text{rank}(\mathbf{S}_p^T[\phi_j \quad \phi_{j+1} \quad \dots \quad \phi_{j+m_l-1}]) = m_l \quad (\text{C.6})$$

The matrix $\mathbf{S}_p^T[\phi_j \quad \phi_{j+1} \quad \dots \quad \phi_{j+m_l-1}]$ in Eq. (C.6) is obtained from the matrix $\mathbf{S}_p^T[q_j \phi_j \quad q_{j+1} \phi_{j+1} \quad \dots \quad q_{j+m_l-1} \phi_{j+m_l-1}]$ in Eq. (C.5) by multiplying each column by a non-zero scaling factor. These column operations do not affect the matrix rank [25].

Appendix D. Proof of Theorem 4.2

A transformation of the state vector $\mathbf{x}_{[k]} \rightarrow \mathbf{T}^{-1} \mathbf{x}_{[k]}$ and the corresponding transformation of the system, as considered in Appendix B, do not affect the system zeros. This is shown next.

The system transmission zeros $\lambda_j \in \mathbb{C}$ of the system obtained after transformation fulfil the following inequality (cfr. Eq. (20)):

$$\text{rank} \left(\begin{bmatrix} \mathbf{T}^{-1} \mathbf{A} \mathbf{T} - \lambda_j \mathbf{I} & \mathbf{T}^{-1} \mathbf{B} \\ \mathbf{G} \mathbf{T} & \mathbf{J} \end{bmatrix} \right) < n_s + \min(n_p, n_d) \quad (\text{D.1})$$

Decomposition of the matrix in Eq. (D.1) yields:

$$\text{rank} \left(\begin{bmatrix} \mathbf{T}^{-1} & \mathbf{0} \\ \mathbf{0} & \mathbf{I}_{n_d} \end{bmatrix} \begin{bmatrix} \mathbf{A} - \lambda_j \mathbf{I} & \mathbf{B} \\ \mathbf{G} & \mathbf{J} \end{bmatrix} \begin{bmatrix} \mathbf{T} & \mathbf{0} \\ \mathbf{0} & \mathbf{I}_{n_p} \end{bmatrix} \right) < n_s + \min(n_p, n_d) \quad (\text{D.2})$$

where $\mathbf{I}_{n_d} \in \mathbb{R}^{n_d \times n_d}$ and $\mathbf{I}_{n_p} \in \mathbb{R}^{n_p \times n_p}$ are identity matrices. The transformation matrix \mathbf{T} is nonsingular. Therefore, Eq. (D.2) holds if and only if:

$$\text{rank} \left(\begin{bmatrix} \mathbf{A} - \lambda_j \mathbf{I} & \mathbf{B} \\ \mathbf{G} & \mathbf{J} \end{bmatrix} \right) < n_s + \min(n_p, n_d) \quad (\text{D.3})$$

This implies that the transmission zeros of the system obtained after transformation under \mathbf{T} equal the transmission zeros of the original system.

For $\mathbf{T} = \mathbf{\Psi}_d$, with $\mathbf{\Psi}_d$ the matrix containing the eigenvectors of \mathbf{A} (see Eq. (A.1)), the decoupled system given by Eqs. (A.2) and (A.3) is obtained, and Eq. (D.1) becomes:

$$\text{rank} \left(\begin{bmatrix} \mathbf{\Lambda}_d - \lambda_j \mathbf{I} & \mathbf{L}_d^T \\ \mathbf{\Phi}_d & \mathbf{J} \end{bmatrix} \right) < n_s + \min(n_p, n_d) \quad (\text{D.4})$$

The system defined by Eqs. (2) and (5) has a transmission zero $\lambda_j = 1$ if and only if:

$$\text{rank} \left(\begin{bmatrix} \mathbf{\Lambda}_d - \mathbf{I} & \mathbf{L}_d^T \\ \mathbf{\Phi}_d & \mathbf{J} \end{bmatrix} \right) < n_s + \min(n_p, n_d) \quad (\text{D.5})$$

Under the assumption that the system does not contain rigid body modes ($\lambda_{d,n} \neq 1$), $\mathbf{\Lambda}_d - \mathbf{I}$ is of full rank, and the following equality holds:

$$\begin{aligned} \text{rank} \left(\begin{bmatrix} \mathbf{\Lambda}_d - \mathbf{I} & \mathbf{L}_d^T \\ \mathbf{\Phi}_d & \mathbf{J} \end{bmatrix} \right) &= \text{rank} \left(\begin{bmatrix} \mathbf{\Lambda}_d - \mathbf{I} & \mathbf{0} \\ \mathbf{0} & \mathbf{J} - \mathbf{\Phi}_d (\mathbf{\Lambda}_d - \mathbf{I})^{-1} \mathbf{L}_d^T \end{bmatrix} \right) \\ &= n_s + \text{rank}(\mathbf{J} - \mathbf{\Phi}_d (\mathbf{\Lambda}_d - \mathbf{I})^{-1} \mathbf{L}_d^T) \end{aligned} \quad (\text{D.6})$$

Time discretization of the system does not change the response of the system to excitation which is constant in time ($\omega = 0$ rad/s, $\lambda = 1$) [30]. Therefore, any input $\mathbf{p}_{[k]} = \mathbf{p}$, with $\mathbf{p} \in \mathbb{R}^{n_p}$ an arbitrary vector which does not depend on the time step k , yields zero velocities and accelerations at steady state: $\mathbf{d}_{[k]} = \mathbf{0}$, $\mathbf{x}_{m[k+1]} = \mathbf{x}_{m[k]}$. For the case of excitation which is constant in time ($\mathbf{p}_{[k]} = \mathbf{p}$), elaboration of Eqs. (A.2) and (A.3) yields:

$$\mathbf{J} - \Phi_d(\Lambda_d - \mathbf{I})^{-1}\mathbf{L}_d^T = \mathbf{0} \quad (\text{D.7})$$

From Eqs. (D.6) and (D.7) it follows that:

$$\text{rank} \left(\begin{bmatrix} \Lambda_d - \mathbf{I} & \mathbf{L}_d^T \\ \Phi_d & \mathbf{J} \end{bmatrix} \right) = n_s < n_s + \min(n_p, n_d) \quad (\text{D.8})$$

with $n_p > 0$ and $n_d > 0$. This shows that $\lambda_j = 1$ is a transmission zero of the system defined by Eqs. (2) and (5) if the output vector $\mathbf{d}_{[k]}$ only contains acceleration and/or velocity measurements.

Appendix E. Proof of Theorem 4.3

In Appendix D it is found that the system defined by Eqs. (2) and (5) has a transmission zero $\lambda_j = 1$ if and only if Eq. (D.5) holds. Taking into account Eq. (D.6) and assuming that none of the modes is a rigid body mode characterized by $\omega_{d,j} = 0$ rad/s, it follows that in order to avoid transmission zeros $\lambda_j = 1$, the following equation must hold:

$$\text{rank}(\mathbf{J} - \Phi_d(\Lambda_d - \mathbf{I})^{-1}\mathbf{L}_d^T) \geq \min(n_p, n_d) \quad (\text{E.1})$$

Taking into account that $\Lambda_d = \Psi_d \mathbf{A} \Psi_d^{-1}$, $\mathbf{L}_d^T = \Psi_d \mathbf{B}$, and $\Phi_d = \mathbf{G} \Psi_d^{-1}$, it can be shown that:

$$\text{rank}(\mathbf{J} - \Phi_d(\Lambda_d - \mathbf{I})^{-1}\mathbf{L}_d^T) = \text{rank}(\mathbf{J} - \mathbf{G}(\mathbf{A} - \mathbf{I})^{-1}\mathbf{B}) \quad (\text{E.2})$$

Since the rank of a matrix cannot be larger than any of its dimensions (i.e. $\text{rank}(\mathbf{J} - \mathbf{G}(\mathbf{A} - \mathbf{I})^{-1}\mathbf{B}) \leq \min(n_p, n_d)$), it can be concluded that transmission zeros of a system corresponding to a frequency of 0 Hz ($\lambda_j = 1$) can be avoided by requiring that $\text{rank}(\mathbf{J} - \mathbf{G}(\mathbf{A} - \mathbf{I})^{-1}\mathbf{B}) = \min(n_p, n_d)$.

Appendix F. Proof of Proposition 4.1

From Eq. (E.2) it is found that $\text{rank}(\mathbf{J} - \mathbf{G}(\mathbf{A} - \mathbf{I})^{-1}\mathbf{B}) = \min(n_p, n_d)$ if and only if:

$$\text{rank}(\mathbf{J} - \Phi_d(\Lambda_d - \mathbf{I})^{-1}\mathbf{L}_d^T) = \min(n_p, n_d) \quad (\text{F.1})$$

The n_d rows of the matrix $\mathbf{J} - \Phi_d(\Lambda_d - \mathbf{I})^{-1}\mathbf{L}_d^T$ can be split in (1) $n_{d,a} + n_{d,v}$ rows corresponding to acceleration and velocity measurements, and (2) $n_{d,d}$ rows corresponding to displacement/strain measurements, with $n_d = n_{d,a} + n_{d,v} + n_{d,d}$, where n_d is the total number of output measurements, and $n_{d,a}$, $n_{d,v}$, and $n_{d,d}$ are the number of acceleration, velocity, and displacement/strain measurements, respectively. The $n_{d,a} + n_{d,v}$ rows of the matrix $\mathbf{J} - \Phi_d(\Lambda_d - \mathbf{I})^{-1}\mathbf{L}_d^T$ corresponding to the acceleration and velocity measurements are all zero, since Eq. (D.7) holds. As the rank of a matrix cannot be larger than any of its dimensions and the $n_{d,a} + n_{d,v}$ zero rows do not contribute to the matrix rank, the following equation holds:

$$\text{rank}(\mathbf{J} - \Phi_d(\Lambda_d - \mathbf{I})^{-1}\mathbf{L}_d^T) \leq \min(n_p, n_{d,d}) \quad (\text{F.2})$$

Since the presence of transmission zeros corresponding to a frequency of 0 Hz are associated with acceleration or velocity measurements, $n_{d,a} + n_{d,v} > 0$, and $n_d > n_{d,d}$. From Eq. (F.2) it is found that, for $n_d > n_{d,d}$, Eq. (F.1) can only hold if $n_{d,d} \geq n_p$.